

Quantum path integral molecular dynamics simulations on transport properties of dense liquid helium

Dongdong Kang, Jiayu Dai, Huayang Sun

Department of Physics, College of Science, National University of Defense Technology,
Changsha 410073, Hunan, People's Republic of China

`jydai@nudt.edu.cn`

and

Jianmin Yuan

Department of Physics, College of Science, National University of Defense Technology,
Changsha 410073, Hunan, People's Republic of China

IFSA Collaborative Innovation Center, Shanghai Jiao Tong University, Shanghai 200240,
People's Republic of China

`jmyuan@nudt.edu.cn`

Received _____; accepted _____

ABSTRACT

Transport properties of dense liquid helium under the conditions of planet's core and cool atmosphere of white dwarfs have been investigated by using the improved centroid path-integral simulations combined with density functional theory. The self-diffusion is largely higher and the shear viscosity is notably lower predicted with the quantum mechanical description of the nuclear motion compared with the description by Newton equation. The results show that nuclear quantum effects (NQEs), which depends on the temperature and density of the matter via the thermal de Broglie wavelength and the ionization of electrons, are essential for the transport properties of dense liquid helium at certain astrophysical conditions. The Stokes-Einstein relation between diffusion and viscosity in strongly coupled regime is also examined to display the influences of NQEs.

Subject headings: dense matter - dense helium - diffusion - viscosity - quantum effects

1. Introduction

Helium, the second most abundant element in the universe, is one of the main components of giant planets and a large number of recently discovered exoplanets (Santos et al. 2005; McMahan et al. 2012). Meanwhile, helium is also expected to be largely present in the cool white dwarf atmospheres (Winisdoerffer & Chabrier 2005), which generally affect the cooling rate of white dwarfs (WDs) when having exhausted their nuclear fuel. Matter in these astrophysical bodies is generally under extreme temperature and pressure conditions (Chabrier et al. 2007). For instance, the temperature range of Jupiter, a typical solar giant planet, is estimated from 6500 K to 20000 K, while the pressure can reach 70 Mbar (Fortov 2011). For some exoplanets, it can be up to 19 Gbar (Swift et al. 2012). The density range of the outer layer of WDs is a few g/cm^3 and the temperature retains thousands of Kelvin (Iglesias et al. 2002). The central element for determining the structure and evolution of these astrophysical objects is the accurate description of the physical properties of matter under the relevant conditions of temperature and pressure (Fortney & Nettelmann 2010; Kang et al. 2011, 2013; French et al. 2012; Militzer 2013), which includes transport properties of the characteristic materials. In fact, atomic diffusion, as a basic physical process, plays a significant role in modeling the interior evolution of astrophysical objects (Michaud et al. 2007). Therefore, the physical properties of helium under extreme conditions is of continuous and strong interest owing to the aforementioned wealth applications to astrophysics (Fortov 2011).

Despite the simplicity of atomic structure, bulk helium exhibits complex behavior, especially under astrophysical conditions because the states cover from atomic, partially ionized to fully ionized helium (Kietzmann et al. 2007; Khairallah & Militzer 2008; Stixrude & Jeanloz 2008; McMahan et al. 2012). In past few decades, great progresses have been achieved to explore the physics of helium at extreme states experimentally, such as diamond

anvil cell and shock wave (Celliers et al. 2010; Soubiran et al. 2012). However, only narrow bands of temperature and pressure parameters attainable by laboratory measurements today. Thus the comprehensive understanding of helium at extreme states requires accurate theoretical calculations. Conventional approaches that are suitable for treating ideal plasma gas or condensed matter under ambient conditions usually fail to solve the issues in the warm dense regime (Graziani et al. 2014). Ab initio approaches based on density functional theory (DFT) provide a feasible and satisfactory tool to investigate the physical properties of matter under extreme conditions. They have been extensively used to obtain the thermodynamical, transport, and optical properties of matter in astrophysical area (French et al. 2012). Quantum Langevin molecular dynamics (QLMD), including non-adiabatic effects such as the electron-ion collision induced friction in molecular dynamics (Dai et al. 2010a), extends the quantum molecular dynamics to the regime up to solar interior (Dai et al. 2010b, 2012, 2013).

A common feature of these theoretical methods is that the ions are treated classically, that is, the quantum nature of ions motion is neglected. It should be noted that due to the low mass, helium motion is expected to be fairly sensitive to quantum effects, the so-called nuclear quantum effects (NQE), as hydrogen exhibits (Kang et al. 2014). The well-known superfluidity of helium is dominated by quantum effects of helium atoms at extremely low temperatures (Ceperley 1995). At relatively high temperatures in planet’s core or outer layer of WDs, NQEs are usually considered to be negligible before. Note that with the increasing density of helium, the atomic distance decreases. When the nearest atomic distance is comparable to the thermal de Broglie wavelength, the nuclear quantum delocalization would play remarkable roles in structure and transport properties, e.g., NQEs induce complex transport behavior in warm dense hydrogen as reported in our previous work (Kang et al. 2014). Path-integral molecular dynamics is an effective tool to investigate the NQEs on static properties of extreme states (Marx & Parrinello 1996) and recently

improved centroid path-integral molecular dynamics (PIMD) can provide the well-defined quasiclassical approximation of real-time evolution of quantum systems (Cao & Voth 1993; Kang et al. 2014). Therefore, centroid PIMD, combined with DFT, treats both electrons and ions quantum-mechanically. Using this method, more accurate description of transport properties of matter at extreme states is expected to be obtained.

In this study, we investigate NQEs on the structural and transport properties of dense liquid helium at 5 g/cm³ and 10 g/cm³ using ab initio centroid PIMD with an improved scheme, and compare the results with that from traditional first principles molecular dynamics (MD) calculations based on DFT with a classical treatment of nuclei to assess the importance of NQEs.

2. Theoretical Methods

Path-integral formulation of quantum statistical mechanics provides a theoretical and computational framework to study the quantum many-body system at finite temperatures (Feynman 1972). In path-integral picture, the canonical partition function can be expressed as a configurational integral of Boltzmann weighted continuous paths. If exchange effects of particles are negligible, these closed paths can be discretized through Trotter approximation into P beads circularly connected via harmonic springs, so that a quantum system including N particles is isomorphic to a classical system consisting of N ring polymers, where each quantum particle is mapped onto a closed flexible polymer of P beads (Parrinello & Rahman 1984; Marx & Parrinello 1996). Static properties, e.g., radial distribution function (RDF), of the quantum system are routinely obtained through molecular dynamics sampling the configuration space of its isomorphic classical system. Further, centroid molecular dynamics within the framework of path-integral improved recently is a good quasiclassical approximation to quantum dynamics (Kang et al. 2014). In the adiabatic centroid PIMD

scheme (Marx et al. 1999), the primitive path variables $\{\mathbf{R}_I\}^{(s)}$ (s is the imaginary time.) is transformed to a set of normal mode variables $\{\mathbf{y}_I\}^{(s)}$, which diagonalize the harmonic bead coupling. The equations of motion of normal mode variables without thermostats are given by

$$M_I^{(1)}\ddot{\mathbf{y}}_I^{(1)} = -\frac{\partial}{\partial \mathbf{y}_I^{(1)}} \frac{1}{P} \sum_{s=1}^P E^{(s)}, \quad (1)$$

$$M_I^{(s)}\ddot{\mathbf{y}}_I^{(s)} = -\frac{\partial}{\partial \mathbf{y}_I^{(s)}} \frac{1}{P} \sum_{s'=1}^P E^{(s')} - M_I^{(s)}\omega_P^2 \mathbf{y}_I^{(s)}, \quad s = 2, \dots, P, \quad (2)$$

where $\omega_P = \sqrt{P}k_B T$, P is the number of beads in ring polymer, k_B is Boltzmann constant, T is the target temperature of the simulated system, $E^{(s)}$ is the electronic energy functional in *ab initio* calculations.

The centroid and non-centroid modes are mass-scale separated with adiabatic parameter γ , i. e., the normal mode masses $M_I^{(s)}$ are

$$M_I^{(1)} = M_I, \quad M_I^{(s)} = \gamma M_I^{(s)}, \quad s = 2, \dots, P. \quad (3)$$

where M_I is the physical nuclear mass. In this way, the nuclear quantum dynamics is obtained in the quasiclassical approximation through driving the centroid move in real-time in the centroid effective potential generated by all non-centroid modes. Here we propose a new scheme for sampling the force on the centroids during the molecular dynamics simulations to make the size of ring polymer is more close to the de Broglie wavelength as the instantaneous kinetic energy of ions is decreased. That is, for each ion ω_P depend linearly on its instantaneous kinetic energy $E(t)$ during simulations,

$$\omega_P(t) = \frac{2N}{g} \sqrt{P} (aE(t) + bE_0), \quad (4)$$

where t is the simulation time step. The details of determining the parameters a and b are given elsewhere (Kang et al. 2014). Here we show the results, i.e., $a = 1 - (\frac{2R_{g0}}{\lambda})^2$ and

$b = (\frac{2R_{g0}}{\lambda})^2$, where R_{g0} is the radius of gyration of ring polymer when $E(t) = E_0$, λ is the de Broglie wavelength of the corresponding ion. As shown in Kang et al. (2014), this improved centroid PIMD approach can describe the quantum collision properly, and nuclear quantum dynamics in dense hydrogen has been investigated successfully.

3. Results and Discussion

3.1. Computational details

For dense helium, we study the structural and transport properties at densities of 5 g/cm³ and 10 g/cm³ above the melting point temperature. The knowledge of the structure and transport properties of dense liquid helium under these density and temperature conditions is essential to correctly describe the interior structure and evolution and cooling of astrophysical bodies, such as exoplanets and outer layer of white dwarfs. Exchange effects between ions are neglected in this study (Dyugaev 1990) because the atomic distance is still larger than the thermal de Broglie wavelength of ions under the conditions considered here.

Our MD and PIMD simulations were performed using the modified Quantum-ESPRESSO package (Giannozzi et al. 2009), where electrons are quantum-mechanically treated by finite-temperature density functional theory (Mermin 1965). The interaction between valence electron and the ionic core is presented by norm-conserving pseudopotential. The generalized-gradient approximation for exchange-correlation potential (Perdew et al. 1996) is adopted. The plane-wave kinetic energy cutoff was set from 150 to 180 Ry according to different densities. The Brillouin zone is sampled using the Gamma point in dynamic simulations, while denser k-point grids of 4×4×4 Monkhorst-Pack scheme points are used to calculate electronic properties. The periodic supercell including 128 or 250 atoms is adopted for 5 g/cm³ and 10 g/cm³, which can ensure convergence of both ionic

and electronic properties with good accuracy.

Within the framework of PIMD, the structural properties are calculated using the primitive scheme, while the real-time quantum dynamics of nuclei is obtained through the improved centroid PIMD. The self-diffusion coefficient is calculated from the slope of the centroid mean square displacement, while the shear viscosity is obtained from the autocorrelation function of the off-diagonal components of the stress tensor (Alfè & Gillan 1998). Langevin thermostat is employed to overcome the nonergodic problem, which not only produces a canonical ensemble and compensates the calculated errors, but also gives an good method to include the non-adiabatic effects of electrons in warm and hot dense regime (Dai et al. 2010a,b). Note that Langevin thermostat is applied only to each noncentroid degree of freedom because large thermostats would disturb the dynamical properties of the centroids. The Trotter number was set to 16 after a convergence test. Time step of 7-9 a.u. is used in the MD calculations with 30000 steps after thermalization, while the smaller time steps of 0.3 a.u. with 5×10^5 steps and a centroid adiabaticity parameter of 20 are adopted in the centroid PIMD simulations in order to decouple the centroid mode from other normal modes.

3.2. Transport properties of dense liquid helium

Firstly, we calculated the RDF of helium nuclei to reveal the structural difference introduced by NQEs. Within the framework of imaginary-time PIMD, the quantum expectation value of a static physical quantity is given in terms of averaging over the canonical ensemble of the isomorphic classical system. Therefore, the radial distribution functions of helium atoms are obtained by averaging over both the PIMD time steps and imaginary time slices. Figure 1 shows that NQEs play an important role in RDF at low temperatures with the density range of 5 g/cm³ and 10 g/cm³. In particular, the first peak

of RDF from PIMD simulations are largely reduced and broadened, which indicates the significant nuclear quantum delocalization. When the temperature is increased, the nuclear quantum delocalization becomes weaker and cannot be observed ultimately at 10000 K for 5 g/cm³ helium and 12000 K for 10 g/cm³ helium. Meanwhile, RDF shows more pronounced nuclear quantum effect with increasing density, even though the temperature (7000 K) at 10 g/cm³ is higher than that (4000 K) at 5 g/cm³.

Of our particular interest is NQEs on transport properties of dense liquid helium because atomic diffusion is the basic physical process that determine the interior structure and evolution of astrophysical objects (Michaud et al. 2007). The results of the self-diffusion coefficient and shear viscosity at 5 g/cm³ with the temperature range of 4000-10000 K are shown in Figure 2. When taking into account the quantum features of the collision processes between ions properly, the self-diffusion coefficients obtained by centroid PIMD simulation are substantially larger than the classical simulation value over the whole temperature range of 4000-10000 K. The difference is 37% at 4000 K, 22% at 6000 K, 17% at 8000 K and 10% at 10000 K. It is interesting that even though the RDF from MD and PIMD calculations are almost identical when the temperature is increased to 10000 K, the ionic diffusion still exhibits distinct difference with the inclusion of NQEs. In fact, the essence of atomic diffusion is atomic scattering from the viewpoint of collision physics. The large-angle scattering between ions is dominant under the high density conditions considered here. The pronounced quantum nuclear scattering features introduced by centroid PIMD simulations leads to a smaller large-angle scattering cross section between ions than the classical treatment, thereby increasing the mean free path of ions. Thus the classical-particle treatment of protons substantially underestimates the ionic diffusion. Similarly, the self-diffusion coefficients at the temperature range of 7000-12000 K from quantum simulations for helium at 10 g/cm³, as shown in Figure 3, are 23 %, 21 %, 12 % and 6 % higher than that from classical simulations.

The shear viscosities calculated from the Green-Kubo relation (Alfè & Gillan 1998) at the density of 5 g/cm³ and 10 g/cm³ are also shown in Figure 2 and 3, respectively. We can see that the viscosities from centroid PIMD are smaller than those from MD and the difference between them becomes smaller with increasing temperatures. In addition to obtaining the viscosity from molecular dynamics simulations, it can be alternatively deduced from the Stokes-Einstein (SE) relation with slip or stick boundary conditions (Hansen & McDonald 2011). The SE relation, which is exact for the Brownian particles, is not valid in strongly coupled regime. In order to examine the SE relation, we calculated the parameter $D\eta a/k_B T$ (a is the effective atomic diameter and defined by the position of the first peak of RDF) and the results are shown in Figure 2 and 3 for the density of 5 g/cm³ and 10 g/cm³, respectively. The parameter $D\eta a/k_B T$ both from MD and PIMD calculations deviates from the SE relation value $1/2\pi$ at low temperatures; furthermore, NQEs introduce pronounced difference between the classical and quantum simulations. In fact, the state of helium in planet’s core or cool atmosphere of WDs is in moderately or strongly coupled regime and the motion of ions is quite different from Brownian motion.

In order to understand the atomic diffusion behavior with NQEs microscopically, we explore the potential surface of a randomly selected atom along its simulation trajectory. Given the force in simulations is calculated by $\mathbf{F} = -\nabla V$, the potential energy along the trajectory of a atom can be obtained by $V = V_0 + \int \mathbf{F} \cdot d\mathbf{r}$, where \mathbf{F} is the force acting on atoms, V is the potential energy, V_0 is the reference point of potential energy. The potential energy of a randomly selected helium atom along its simulation trajectory from MD and PIMD simulations as well as the distribution of the potential energy is presented in Figure 4. We can see that in PIMD simulations the potential energy of the imaginary-time beads fluctuates steeply, which presents the effects of quantum fluctuations on dynamics of the centroid. The potential surface of the centroid exhibits more smoothly than that of classical particle, which is evidenced by the fact that the distribution of the potential

energy of centroid covers smaller energy range than MD simulation and the high frequency component of the potential surface of the centroid is higher than MD results by about 100 THz for both 5 g/cm³ and 10 g/cm³, as shown in Figure 4(c) and (f). It indicates that when considering NQEs the atoms are more prone to turn over the energy barrier than classical treatment, thereby enhancing the atomic diffusion. In addition, it is shown in Figure 4 that when the density is increased from 5 g/cm³ to 10 g/cm³, the potential surface exhibits more barriers and wells in the same range of time (100 fs) both in MD and PIMD simulations. It unambiguously indicates that helium atoms collide more frequently at higher density at the same temperature so that the atomic diffusion is lowered at high densities.

Nuclear motion quantum nature not only affect the atomic diffusion behavior, but also induce the electronic redistribution (Cannuccia & Marini 2011), thus introducing more localized electrons (Kang et al. 2013, 2014). It can be evidenced by the distribution of charge density shown in Figure 5. Note that with the inclusion of NQEs, the charge density has the larger maxima and smaller minima compared with the classical simulations, which indicates that electrons surrounding ions distribute more localized with quantum nuclei than classical particle treatment. For metallic state of matter, e.g., dense hydrogen, this electronic localization can significantly lower the dc electrical and thermal conductivities (Kang et al. 2014). For dense liquid helium, NQEs induce a strong impact on the electronic density of states (DOS). We can see from Figure 6 that the energy bands, especially conduction bands are obviously broadened when NQEs are considered via PIMD. Since helium exhibits a large electronic energy gap under the conditions considered here, it is still in insulator state. Therefore, NQEs on electronic transport properties are not discussed here. Except for NQEs on DOS, density effect has also influenced the profile of DOS remarkably. As shown in Figure 6, when the density of helium is increased from 5 g/cm³ to 10 g/cm³, the energy gap is decreased, thus the *K*-edge photo-absorption spectra will have a red shift. More importantly, we note that the DOS of the 1s state is extended by about

30 eV when helium is compressed from 5 g/cm^3 to 10 g/cm^3 , which significantly affects the interaction potential between helium nuclei and make the potential surface fluctuates more frequently at high density (shown in Figure 4). Therefore, both NQEs and density effect contributes to the complex transport properties of atoms.

4. Conclusion

In conclusion, NQEs on transport properties of dense liquid helium under the conditions of the planet's core and cool atmosphere of WDs have been investigated using the improved centroid PIMD simulations combining with DFT. The results show that with the inclusion of NQEs, the self-diffusion is largely higher while the shear viscosity is notably lower than the results of without the inclusion of NQEs due to the lower collision cross sections even when the NQEs have little effects on the static structures. Meanwhile, the relation between diffusion and viscosity is deviate from the SE relation valid for Brownian particles, thus the SE relation is not valid in strongly coupled regime. The potential surface of helium atom along the simulation trajectory is quite different between MD and PIMD simulations. We have shown that the quantum nuclear character induces complex behaviors for ionic transport properties of dense liquid helium. Therefore, in order to construct more reasonable structure and evolution model for the planets and WDs, NQEs must be reconsidered when calculating the transport properties at certain temperature and density conditions.

This work is supported by the National Basic Research Program of China (973 Program) under Grant No. 2013CB922203, the National Natural Science Foundation of China under Grant Nos. 11422432, 11274383 and 61221491. DJY thanks the support by the Advanced Research Foundation of National University of Defense Technology. Calculations were carried out at the Research Center of Supercomputing Application, NUDT.

REFERENCES

- Alfè, D., & Gillan, M. J. 1998, *Phys. Rev. Lett.*, 81, 5161
- Cao, J., & Voth, G. A. 1993, *J. Chem. Phys.*, 99, 10070
- Cannuccia, E., & Marini, A. 2011, *Phys. Rev. Lett.*, 107, 255501
- Celliers, P. M., Loubeyre, P., Eggert, J. H., et al. 2010, *Phys. Rev. Lett.*, 104, 184503
- Ceperley, D. M. 1995, *Rev. Mod. Phys.*, 67, 279
- Chabrier, G., Saumon, D., & Winisdoerffer, C. 2007, *Astrophys. Space Sci.*, 307, 263
- Dai, J., Hou, Y., & Yuan, J. 2010a, *Phys. Rev. Lett.*, 104, 245001
- Dai, J., Hou, Y., & Yuan, J. 2010b, *ApJ*, 721, 1158
- Dai, J., Kang, D., Zhao, Z., Wu, Y., & Yuan, J. 2012, *Phys. Rev. Lett.*, 109, 175701
- Dai, J., Hou, Y., Kang, D., et al. 2013, *New J. Phys.*, 15, 045003
- Dyugaev, A. M. 1990, *J. Low Temp. Phys.*, 78, 79
- Feynman, R. P. 1972, *Statistical Mechanics* (New York: Benjamin)
- Fortney, J. J., & Nettelmann, N. 2010, *Space Sci. Rev.*, 152, 423
- Fortov, V. E. 2011, *Extreme States of Matter* (Berlin: Springer)
- French, M., Becker, A., Lorenzen, W., et al. 2012, *ApJS*, 202, 5
- Giannozzi, P., et al. 2009, *J. Phys.: Condens. Matter*, 21, 395502
- Graziani, F., Desjarlais, M. P., Redmer, R., & Trickey, S. B. 2014, *Frontiers and Challenges in Warm Dense Matter* (Heidelberg: Springer)

- Hansen, J.-P., & McDonald, I. R. 2011, *Theory of Simple Liquids* (Academic Press)
- Holst, B., French, M., & Redmer, R. 2011, *Phys. Rev. B*, 83, 235120
- Iglesias, C. A., Rogers, F. J., & Saumon, D. 2002, *ApJ*, 569, L111
- Kang, D., Dai, J., & Yuan, J. 2011, *J. Chem. Phys.*, 135, 024505
- Kang, D., Dai, J., Sun, H., Hou, Y., & Yuan, J. 2013, *Sci. Rep.*, 3, 3272
- Kang, D., Sun, H., Dai, J., et al. 2014, *Sci. Rep.*, 4, 5484
- Khairallah, S. A., & Militzer, B. 2008, *Phys. Rev. Lett.*, 101, 106407
- Kietzmann, A., Holst, B., & Redmer, R. 2007, *Phys. Rev. Lett.*, 98, 190602
- Marx, D., & Parrinello, M. 1996, *J. Chem. Phys.*, 104, 4077
- Marx, D., Tuckerman, M. E., & Martyna, G. J. 1999, *Comput. Phys. Commun.* 118, 166
- McMahon, J. M., Morales, M. A., Pierleoni, C., & Ceperley, D. M. 2012, *Rev. Mod. Phys.*, 84, 1607
- Mermin, N. D. 1965, *Phys. Rev.*, 137, A1441
- Michaud, G., Richer, J., & Richard, O. 2007, *ApJ*, 670, 1178
- Militzer, B. 2013, *Phys. Rev. B*, 87, 014202
- Parrinello, M., & Rahman, A. 1984, *J. Chem. Phys.*, 80, 860
- Perdew, J. P., Burke, K., & Ernzerhof, M. 1996, *Phys. Rev. Lett.*, 77, 3865
- Santos, N. C., Benz, W., & Mayor, M. 2005, *Science*, 310, 251
- Soubiran, F., Mazevet, S., Winisdoerffer, C., & Chabrier, G. 2012, *Phys. Rev. B*

Stixrude, L., & Jeanloz, R. 2008, Proc. Natl. Acad. Sci. USA, 105, 11071

Swift, D. C., Eggert, J. H., Hicks, D. G., Hamel, S., Caspersen, K., Schwegler, E., Collins, G. W., Nettelmann, N. & Ackland, G. J. 2012, ApJ, 744, 59

Winisdoerffer, C. & Chabrier, G. 2005, Phys. Rev. E, 71, 026402

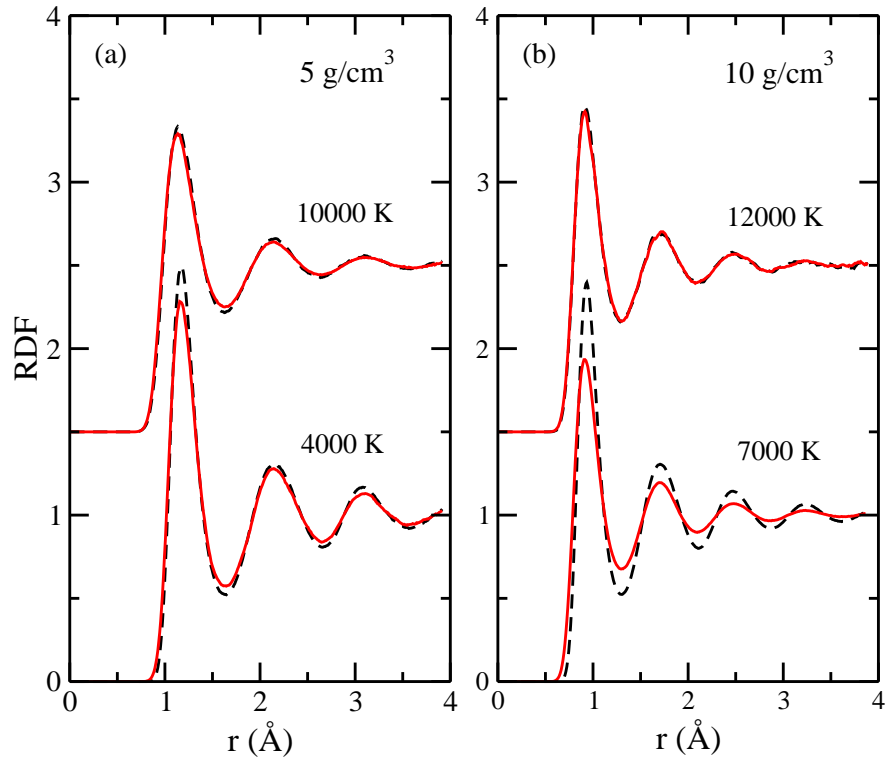


Fig. 1.— Radial distribution functions of helium nuclei from PIMD (solid lines) and MD (dashed lines) simulations with different temperatures at 5 g/cm³ (a) and 10 g/cm³ (b).

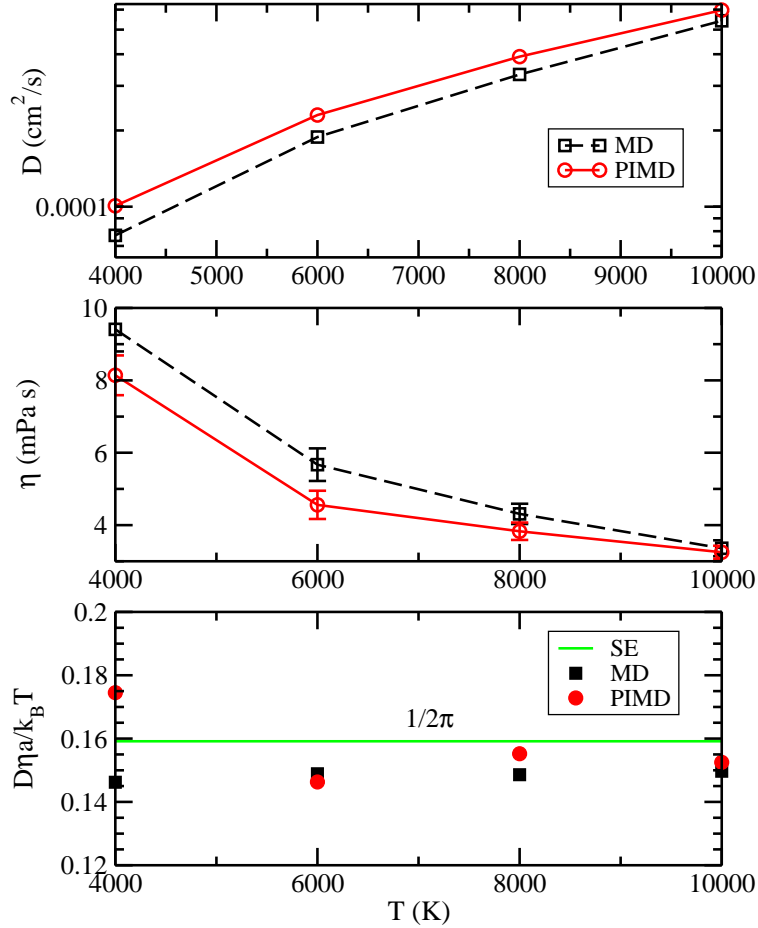


Fig. 2.— Temperature dependence of the self-diffusion coefficient and shear viscosity at 5 g/cm^3 with temperatures of 4000 K, 6000K, 8000 K and 10000 K. obtained from centroid PIMD and MD simulations. The shear viscosities obtained from the Stokes-Einstein (SE) relation are also presented. The effective atomic diameter in SE relation is defined by the position of the first peak of radial distribution function.

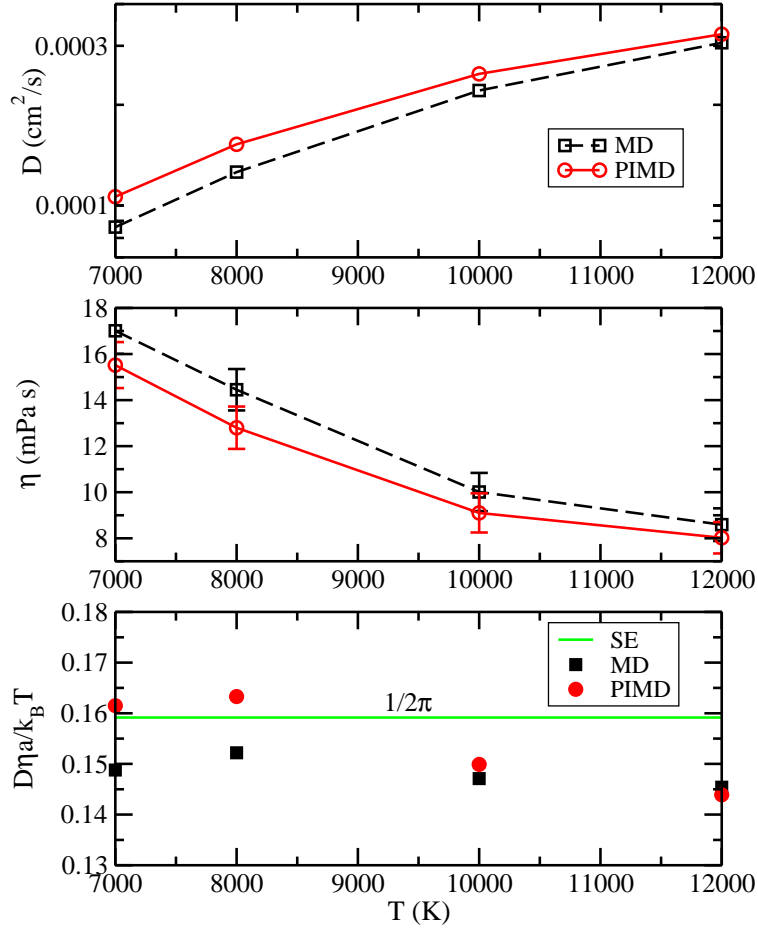


Fig. 3.— Temperature dependence of the self-diffusion coefficient and shear viscosity at 10 g/cm³ with temperatures of 7000 K, 8000K, 10000 K and 12000 K. obtained from centroid PIMD and MD simulations. The shear viscosities obtained from the Stokes-Einstein (SE) relation are also presented. The effective atomic diameter in SE relation is defined by the position of the first peak of radial distribution function.

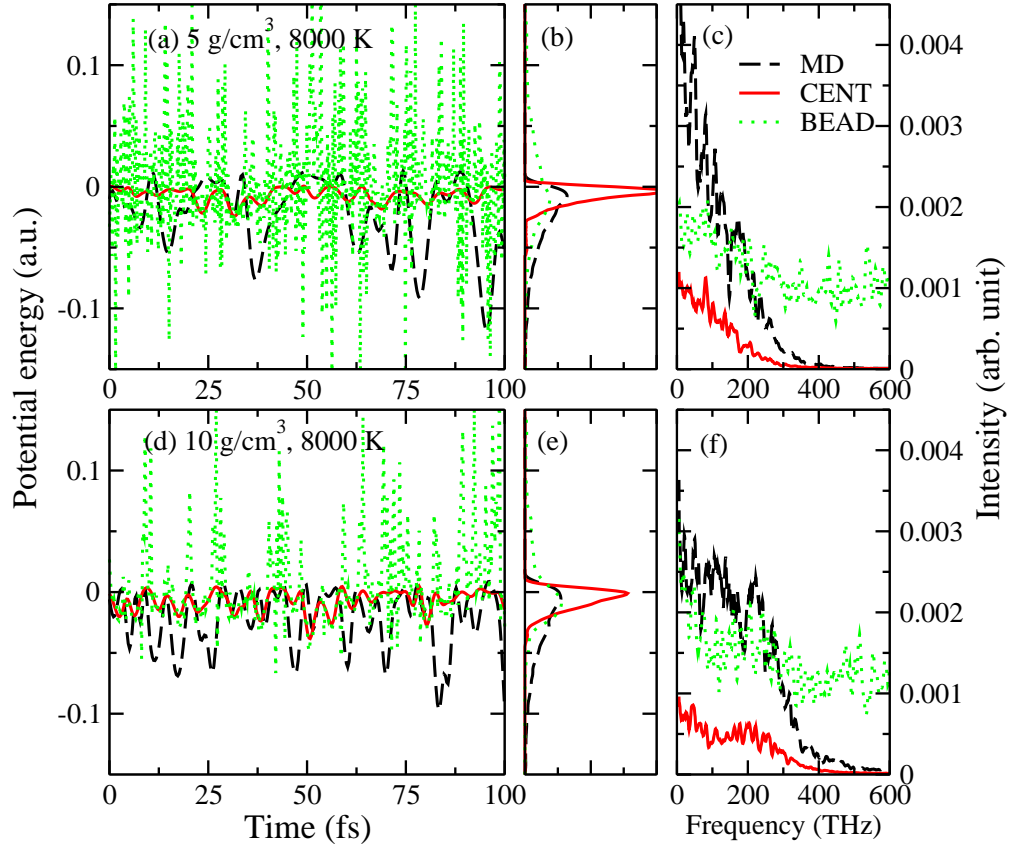


Fig. 4.— The potential energy of a randomly selected helium atom along its simulation trajectory. The results of classical simulation (dashed lines), the centroid of PIMD (solid lines) and the randomly-selected bead in ring polymer (dotted lines) are displayed in two conditions of (5 g/cm^3 , 8000 K) and (10 g/cm^3 , 8000 K). Middle panels (b) and (e) are the distribution of the potential energy. Note that the peaks of distributions are shifted to the same value for comparisons. Right panels (c) and (f) are the fourier transform of the potential surface.

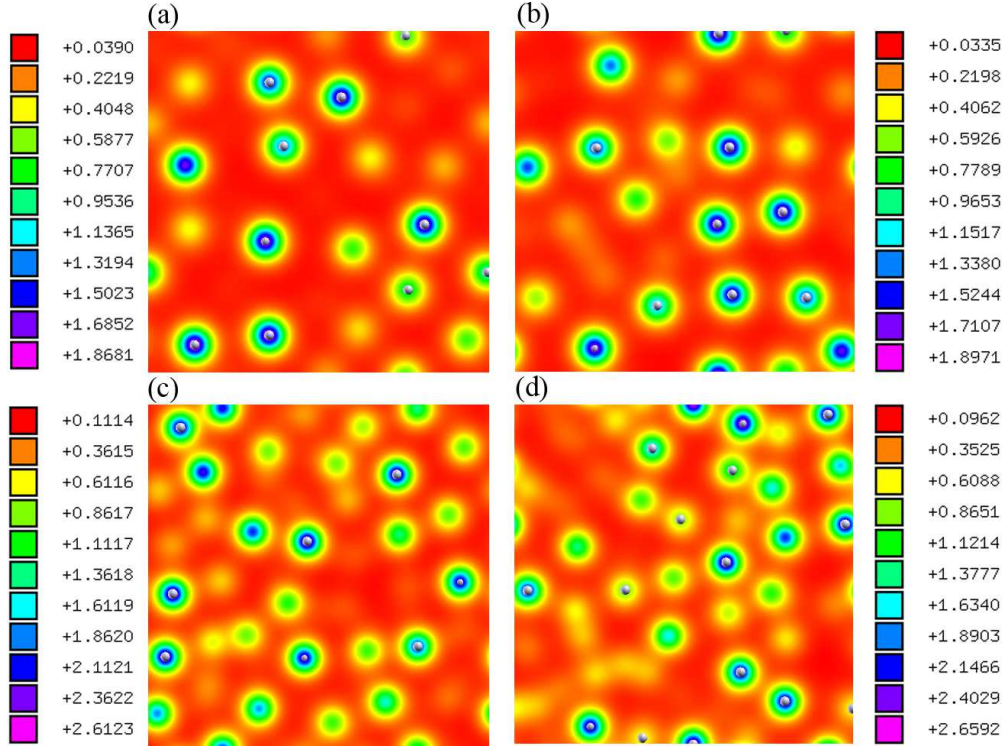


Fig. 5.— The cut-plane of 3D distribution of charge density of randomly selected configurations from MD (a, c) and PIMD (b, d) simulations. For upper panel, the density is 5 g/cm³ and the temperature is 4000 K. For lower panel, the density is 10 g/cm³ and the temperature is 7000 K. In PIMD calculations, the configuration is randomly selected from imaginary-time slices in simulation time steps.

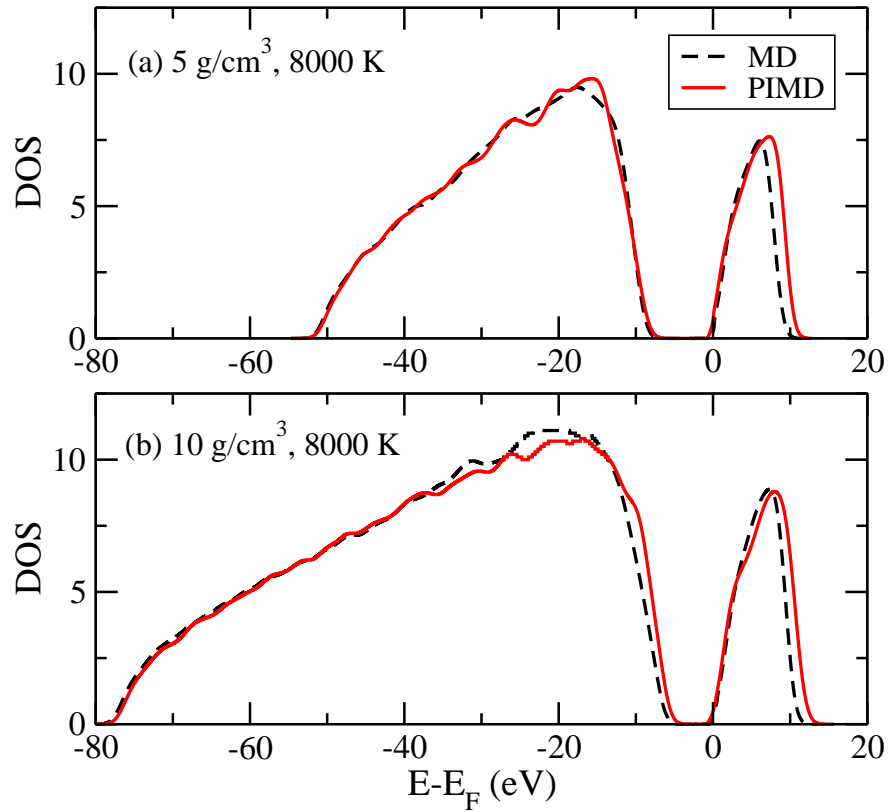


Fig. 6.— The electronic density of states (DOS) calculated from quantum (solid lines) and classical simulations (dashed lines) at 5 g/cm^3 (a) and 10 g/cm^3 (b). The results from PIMD are averaged over not only the simulation time step but also the imaginary-time slices in each simulation time step.